

Determination of strong-phase parameters in $D \rightarrow K_{S,L}^0 \pi^+ \pi^-$

M. Ablikim¹, M. N. Achasov^{10,d}, P. Adlarson⁵⁹, S. Ahmed¹⁵, M. Albrecht⁴, M. Alekseev^{58A,58C}, D. Ambrose⁵¹, A. Amoroso^{58A,58C}, F. F. An¹, Q. An^{55,43}, Anita²¹, Y. Bai⁴², O. Bakina²⁷, R. Baldini Ferroli^{23A}, I. Balossino^{24A}, Y. Ban^{35,l}, K. Begzsuren²⁵, J. V. Bennett⁵, N. Berger²⁶, M. Bertani^{23A}, D. Bettoni^{24A}, F. Bianchi^{58A,58C}, J. Biernat⁵⁹, J. Bloms⁵², I. Boyko²⁷, R. A. Briere⁵, H. Cai⁶⁰, X. Cai^{1,43}, A. Calcaterra^{23A}, G. F. Cao^{1,47}, N. Cao^{1,47}, S. A. Cetin^{46B}, J. Chai^{58C}, J. F. Chang^{1,43}, W. L. Chang^{1,47}, G. Chelkov^{27,b,c}, D. Y. Chen⁶, G. Chen¹, H. S. Chen^{1,47}, J. Chen¹⁶, J. C. Chen¹, M. L. Chen^{1,43}, S. J. Chen³³, Y. B. Chen^{1,43}, W. Cheng^{58C}, G. Cibinetto^{24A}, F. Cossio^{58C}, X. F. Cui³⁴, H. L. Dai^{1,43}, J. P. Dai^{38,h}, X. C. Dai^{1,47}, A. Dbeysi¹⁵, D. Dedovich²⁷, Z. Y. Deng¹, A. Denig²⁶, I. Denysenko²⁷, M. Destefanis^{58A,58C}, F. De Mori^{58A,58C}, Y. Ding³¹, C. Dong³⁴, J. Dong^{1,43}, L. Y. Dong^{1,47}, M. Y. Dong^{1,43,47}, Z. L. Dou³³, S. X. Du⁶³, J. Z. Fan⁴⁵, J. Fang^{1,43}, S. S. Fang^{1,47}, Y. Fang¹, R. Farinelli^{24A,24B}, L. Fava^{58B,58C}, F. Feldbauer⁴, G. Felici^{23A}, C. Q. Feng^{55,43}, M. Fritsch⁴, C. D. Fu¹, Y. Fu¹, Q. Gao¹, X. L. Gao^{55,43}, Y. Gao⁵⁶, Y. Gao⁴⁵, Y. G. Gao⁶, Z. Gao^{55,43}, B. Garillon²⁶, I. Garzia^{24A}, E. M. Gersabeck⁵⁰, A. Gilman⁵¹, K. Goetzen¹¹, L. Gong³⁴, W. X. Gong^{1,43}, W. Gradl²⁶, M. Greco^{58A,58C}, L. M. Gu³³, M. H. Gu^{1,43}, S. Gu², Y. T. Gu¹³, A. Q. Guo²², L. B. Guo³², R. P. Guo³⁶, Y. P. Guo²⁶, A. Guskov²⁷, S. Han⁶⁰, X. Q. Hao¹⁶, F. A. Harris⁴⁸, K. L. He^{1,47}, F. H. Heinsius⁴, T. Held⁴, Y. K. Heng^{1,43,47}, M. Himmelreich^{11,g}, Y. R. Hou⁴⁷, Z. L. Hou¹, H. M. Hu^{1,47}, J. F. Hu^{38,h}, T. Hu^{1,43,47}, Y. Hu¹, G. S. Huang^{55,43}, J. S. Huang¹⁶, X. T. Huang³⁷, X. Z. Huang³³, N. Huesken⁵², T. Hussain⁵⁷, W. Ikegami Andersson⁵⁹, W. Imoehl²², M. Irshad^{55,43}, Q. Ji¹, Q. P. Ji¹⁶, X. B. Ji^{1,47}, X. L. Ji^{1,43}, H. L. Jiang³⁷, X. S. Jiang²⁹, X. Y. Jiang³⁴, J. B. Jiao³⁷, Z. B. Jiao¹⁸, D. P. Jin^{1,43,47}, S. Jin³³, Y. Jin⁴⁹, T. Johansson⁵⁹, N. Kalantar-Nayestanaki²⁹, X. S. Kang³¹, R. Kappert²⁹, M. Kavatsyuk²⁹, B. C. Ke¹, I. K. Keshk⁴, A. Khoukaz⁵², P. Kiese²⁶, R. Kiuchi¹, R. Kliemt¹¹, L. Koch²⁸, O. B. Kolcu^{46B,f}, B. Kopf⁴, M. Kuemmel⁴, M. Kuessner⁴, A. Kupsc⁵⁹, M. Kurth¹, M. G. Kurth^{1,47}, W. Kühn²⁸, J. S. Lange²⁸, P. Larin¹⁵, L. Lavezzi^{58C}, H. Leithoff²⁶, T. Lenz²⁶, C. Li⁵⁹, Cheng Li^{55,43}, D. M. Li⁶³, F. Li^{1,43}, F. Y. Li^{35,l}, G. Li¹, H. B. Li^{1,47}, H. J. Li^{9,j}, J. C. Li¹, J. W. Li⁴¹, Ke Li¹, L. K. Li¹, Lei Li^{3,53}, P. L. Li^{55,43}, P. R. Li³⁰, Q. Y. Li³⁷, W. D. Li^{1,47}, W. G. Li¹, X. H. Li^{55,43}, X. L. Li³⁷, X. N. Li^{1,43}, Z. B. Li⁴⁴, Z. Y. Li⁴⁴, H. Liang^{55,43}, H. Liang^{1,47}, Y. F. Liang⁴⁰, Y. T. Liang²⁸, G. R. Liao¹², L. Z. Liao^{1,47}, J. Libby²¹, C. X. Lin⁴⁴, D. X. Lin¹⁵, Y. J. Lin¹³, B. Liu^{38,h}, B. J. Liu¹, C. X. Liu¹, D. Liu^{55,43}, D. Y. Liu^{38,h}, F. H. Liu³⁹, Fang Liu¹, Feng Liu⁶, H. B. Liu¹³, H. M. Liu^{1,47}, Huanhuan Liu¹, Huihui Liu¹⁷, J. B. Liu^{55,43}, J. Y. Liu^{1,47}, K. Liu¹, K. Y. Liu³¹, Ke Liu⁶, L. Y. Liu¹³, Q. Liu⁴⁷, S. B. Liu^{55,43}, T. Liu^{1,47}, X. Liu³⁰, X. Y. Liu^{1,47}, Y. B. Liu³⁴, Z. A. Liu^{1,43,47}, Zhiqing Liu³⁷, Y. F. Long^{35,l}, X. C. Lou^{1,43,47}, H. J. Lu¹⁸, J. D. Lu^{1,47}, J. G. Lu^{1,43}, Y. Lu¹, Y. P. Lu^{1,43}, C. L. Luo³², M. X. Luo⁶², P. W. Luo⁴⁴, T. Luo^{9,j}, X. L. Luo^{1,43}, S. Lusso^{58C}, X. R. Lyu⁴⁷, F. C. Ma³¹, H. L. Ma¹, L. L. Ma³⁷, M. M. Ma^{1,47}, Q. M. Ma¹, X. N. Ma³⁴, X. X. Ma^{1,47}, X. Y. Ma^{1,43}, Y. M. Ma³⁷, F. E. Maas¹⁵, M. Maggiora^{58A,58C}, S. Maldaner²⁶, S. Malde⁵³, Q. A. Malik⁵⁷, A. Mangoni^{23B}, Y. J. Mao^{35,l}, Z. P. Mao¹, S. Marcello^{58A,58C}, Z. X. Meng⁴⁹, J. G. Messchendorp²⁹, G. Mezzadri^{24A}, J. Min^{1,43}, T. J. Min³³, R. E. Mitchell²², X. H. Mo^{1,43,47}, Y. J. Mo⁶, C. Morales Morales¹⁵, N. Yu. Muchnoi^{10,d}, H. Muramatsu⁵¹, A. Mustafa⁴, S. Nakhoul^{11,g}, Y. Nefedov²⁷, F. Nerling^{11,g}, I. B. Nikolaev^{10,d}, Z. Ning^{1,43}, S. Nisar^{8,k}, S. L. Niu^{1,43}, S. L. Olsen⁴⁷, Q. Ouyang^{1,43,47}, S. Pacetti^{23B}, Y. Pan^{55,43}, M. Papenbrock⁵⁹, P. Patteri^{23A}, M. Pelizaeus⁴, H. P. Peng^{55,43}, K. Peters^{11,g}, J. Pettersson⁵⁹, J. L. Ping³², R. G. Ping^{1,47}, A. Pitka⁴, R. Poling⁵¹, V. Prasad^{55,43}, H. R. Qi², M. Qi³³, T. Y. Qi², S. Qian^{1,43}, C. F. Qiao⁴⁷, N. Qin⁶⁰, X. P. Qin¹³, X. S. Qin⁴, Z. H. Qin^{1,43}, J. F. Qiu¹, S. Q. Qu³⁴, K. H. Rashid^{57,i}, K. Ravindran²¹, C. F. Redmer²⁶, M. Richter⁴, A. Rivetti^{58C}, V. Rodin²⁹, M. Rolo^{58C}, G. Rong^{1,47}, Ch. Rosner¹⁵, M. Rump⁵², A. Sarantsev^{27,e}, M. Savrie^{24B}, Y. Schelhaas²⁶, K. Schoenning⁵⁹, W. Shan¹⁹, X. Y. Shan^{55,43}, M. Shao^{55,43}, C. P. Shen², P. X. Shen³⁴, X. Y. Shen^{1,47}, H. Y. Sheng¹, X. Shi^{1,43}, X. D. Shi^{55,43}, J. J. Song³⁷, Q. Q. Song^{55,43}, X. Y. Song¹, S. Sosio^{58A,58C}, C. Sowa⁴, S. Spataro^{58A,58C}, F. F. Sui³⁷, G. X. Sun¹, J. F. Sun¹⁶, L. Sun⁶⁰, S. S. Sun^{1,47}, X. H. Sun¹, Y. J. Sun^{55,43}, Y. K. Sun^{55,43}, Y. Z. Sun¹, Z. J. Sun^{1,43}, Z. T. Sun¹, Y. T. Tan^{55,43}, C. J. Tang⁴⁰, G. Y. Tang¹, X. Tang¹, V. Thoren⁵⁹, B. Tsednee²⁵, I. Uman^{46D}, B. Wang¹, B. L. Wang⁴⁷, C. W. Wang³³, D. Y. Wang^{35,l}, K. Wang^{1,43}, L. L. Wang¹, L. S. Wang¹, M. Wang³⁷, M. Z. Wang^{35,l}, Meng Wang^{1,47}, P. L. Wang¹, R. M. Wang⁶¹, W. P. Wang^{55,43}, X. Wang^{35,l}, X. F. Wang¹, X. L. Wang^{9,j}, Y. Wang^{55,43}, Y. Wang⁴⁴, Y. F. Wang^{1,43,47}, Y. Q. Wang¹, Z. Wang^{1,43}, Z. G. Wang^{1,43}, Z. Y. Wang¹, Zongyuan Wang^{1,47}, T. Weber⁴, D. H. Wei¹², P. Weidenkaff²⁶, H. W. Wen³², S. P. Wen¹, U. Wiedner⁴, G. Wilkinson⁵³, M. Wolke⁵⁹, L. H. Wu¹, L. J. Wu^{1,47}, Z. Wu^{1,43}, L. Xia^{55,43}, Y. Xia²⁰, S. Y. Xiao¹, Y. J. Xiao^{1,47}, Z. J. Xiao³², Y. G. Xie^{1,43}, Y. H. Xie⁶, T. Y. Xing^{1,47}, X. A. Xiong^{1,47}, Q. L. Xiu^{1,43}, G. F. Xu¹, J. J. Xu³³, L. Xu¹, Q. J. Xu¹⁴, W. Xu^{1,47}, X. P. Xu⁴¹, F. Yan⁵⁶, L. Yan^{58A,58C}, W. B. Yan^{55,43}, W. C. Yan², Y. H. Yan²⁰, H. J. Yang^{38,h}, H. X. Yang¹, L. Yang⁶⁰, R. X. Yang^{55,43}, S. L. Yang^{1,47}, Y. H. Yang³³, Y. X. Yang¹², Yifan Yang^{1,47}, Z. Q. Yang²⁰, M. Ye^{1,43}, M. H. Ye⁷, J. H. Yin¹, Z. Y. You⁴⁴, B. X. Yu^{1,43,47}, C. X. Yu³⁴, J. S. Yu²⁰, T. Yu⁵⁶, C. Z. Yuan^{1,47}, X. Q. Yuan^{35,l}, Y. Yuan¹, A. Yuncu^{46B,a}, A. A. Zafar⁵⁷, Y. Zeng²⁰, B. X. Zhang¹, B. Y. Zhang^{1,43}, C. C. Zhang¹, D. H. Zhang¹, H. H. Zhang⁴⁴, H. Y. Zhang^{1,43}, J. Zhang^{1,47}, J. L. Zhang⁶¹, J. Q. Zhang⁴, J. W. Zhang^{1,43,47}, J. Y. Zhang¹, J. Z. Zhang^{1,47}, K. Zhang^{1,47}, L. Zhang⁴⁵, L. Zhang³³, S. F. Zhang³³, T. J. Zhang^{38,h}, X. Y. Zhang³⁷, Y. Zhang^{55,43}, Y. H. Zhang^{1,43}, Y. T. Zhang^{55,43}, Yang Zhang¹, Yao Zhang¹, Yi Zhang^{9,j}, Yu Zhang⁴⁷, Z. H. Zhang⁶, Z. P. Zhang⁵⁵, Z. Y. Zhang⁶⁰, G. Zhao¹, J. W. Zhao^{1,43}, J. Y. Zhao^{1,47}, J. Z. Zhao^{1,43}, Lei Zhao^{55,43}, Ling Zhao¹, M. G. Zhao³⁴, Q. Zhao¹, S. J. Zhao⁶³, T. C. Zhao¹, Y. B. Zhao^{1,43}, Z. G. Zhao^{55,43}, A. Zhemchugov^{27,b}, B. Zheng⁵⁶, J. P. Zheng^{1,43}, Y. Zheng^{35,l}, Y. H. Zheng⁴⁷, B. Zhong³², L. Zhou^{1,43}, L. P. Zhou^{1,47}, Q. Zhou^{1,47}, X. Zhou⁶⁰, X. K. Zhou⁴⁷, X. R. Zhou^{55,43}, Xiaoyu Zhou²⁰, Xu Zhou²⁰, A. N. Zhu^{1,47}, J. Zhu³⁴, J. Zhu⁴⁴, K. Zhu¹, K. J. Zhu^{1,43,47}, S. H. Zhu⁵⁴, W. J. Zhu³⁴, X. L. Zhu⁴⁵, Y. C. Zhu^{55,43}, Y. S. Zhu^{1,47}, Z. A. Zhu^{1,47}, J. Zhuang^{1,43}, B. S. Zou¹, J. H. Zou¹

(BESIII Collaboration)

¹ Institute of High Energy Physics, Beijing 100049, People's Republic of China

² Beihang University, Beijing 100191, People's Republic of China

³ Beijing Institute of Petrochemical Technology, Beijing 102617, People's Republic of China

⁴ Bochum Ruhr-University, D-44780 Bochum, Germany

⁵ Carnegie Mellon University, Pittsburgh, Pennsylvania 15213, USA

⁶ Central China Normal University, Wuhan 430079, People's Republic of China

⁷ China Center of Advanced Science and Technology, Beijing 100190, People's Republic of China

⁸ COMSATS University Islamabad, Lahore Campus, Defence Road, Off Raiwind Road, 54000 Lahore, Pakistan

- ⁹ Fudan University, Shanghai 200443, People's Republic of China
- ¹⁰ G.I. Budker Institute of Nuclear Physics SB RAS (BINP), Novosibirsk 630090, Russia
- ¹¹ GSI Helmholtzcentre for Heavy Ion Research GmbH, D-64291 Darmstadt, Germany
- ¹² Guangxi Normal University, Guilin 541004, People's Republic of China
- ¹³ Guangxi University, Nanning 530004, People's Republic of China
- ¹⁴ Hangzhou Normal University, Hangzhou 310036, People's Republic of China
- ¹⁵ Helmholtz Institute Mainz, Johann-Joachim-Becher-Weg 45, D-55099 Mainz, Germany
- ¹⁶ Henan Normal University, Xinxiang 453007, People's Republic of China
- ¹⁷ Henan University of Science and Technology, Luoyang 471003, People's Republic of China
- ¹⁸ Huangshan College, Huangshan 245000, People's Republic of China
- ¹⁹ Hunan Normal University, Changsha 410081, People's Republic of China
- ²⁰ Hunan University, Changsha 410082, People's Republic of China
- ²¹ Indian Institute of Technology Madras, Chennai 600036, India
- ²² Indiana University, Bloomington, Indiana 47405, USA
- ²³ (A)INFN Laboratori Nazionali di Frascati, I-00044, Frascati, Italy; (B)INFN and University of Perugia, I-06100, Perugia, Italy
- ²⁴ (A)INFN Sezione di Ferrara, I-44122, Ferrara, Italy; (B)University of Ferrara, I-44122, Ferrara, Italy
- ²⁵ Institute of Physics and Technology, Peace Ave. 54B, Ulaanbaatar 13330, Mongolia
- ²⁶ Johannes Gutenberg University of Mainz, Johann-Joachim-Becher-Weg 45, D-55099 Mainz, Germany
- ²⁷ Joint Institute for Nuclear Research, 141980 Dubna, Moscow region, Russia
- ²⁸ Justus-Liebig-Universitaet Giessen, II. Physikalisches Institut, Heinrich-Buff-Ring 16, D-35392 Giessen, Germany
- ²⁹ KVI-CART, University of Groningen, NL-9747 AA Groningen, The Netherlands
- ³⁰ Lanzhou University, Lanzhou 730000, People's Republic of China
- ³¹ Liaoning University, Shenyang 110036, People's Republic of China
- ³² Nanjing Normal University, Nanjing 210023, People's Republic of China
- ³³ Nanjing University, Nanjing 210093, People's Republic of China
- ³⁴ Nankai University, Tianjin 300071, People's Republic of China
- ³⁵ Peking University, Beijing 100871, People's Republic of China
- ³⁶ Shandong Normal University, Jinan 250014, People's Republic of China
- ³⁷ Shandong University, Jinan 250100, People's Republic of China
- ³⁸ Shanghai Jiao Tong University, Shanghai 200240, People's Republic of China
- ³⁹ Shanxi University, Taiyuan 030006, People's Republic of China
- ⁴⁰ Sichuan University, Chengdu 610064, People's Republic of China
- ⁴¹ Soochow University, Suzhou 215006, People's Republic of China
- ⁴² Southeast University, Nanjing 211100, People's Republic of China
- ⁴³ State Key Laboratory of Particle Detection and Electronics, Beijing 100049, Hefei 230026, People's Republic of China
- ⁴⁴ Sun Yat-Sen University, Guangzhou 510275, People's Republic of China
- ⁴⁵ Tsinghua University, Beijing 100084, People's Republic of China
- ⁴⁶ (A)Ankara University, 06100 Tandogan, Ankara, Turkey; (B)Istanbul Bilgi University, 34060 Eyup, Istanbul, Turkey; (C)Uludag University, 16059 Bursa, Turkey; (D)Near East University, Nicosia, North Cyprus, Mersin 10, Turkey
- ⁴⁷ University of Chinese Academy of Sciences, Beijing 100049, People's Republic of China
- ⁴⁸ University of Hawaii, Honolulu, Hawaii 96822, USA
- ⁴⁹ University of Jinan, Jinan 250022, People's Republic of China
- ⁵⁰ University of Manchester, Oxford Road, Manchester, M13 9PL, United Kingdom
- ⁵¹ University of Minnesota, Minneapolis, Minnesota 55455, USA
- ⁵² University of Muenster, Wilhelm-Klemm-Str. 9, 48149 Muenster, Germany
- ⁵³ University of Oxford, Keble Rd, Oxford, UK OX13RH
- ⁵⁴ University of Science and Technology Liaoning, Anshan 114051, People's Republic of China
- ⁵⁵ University of Science and Technology of China, Hefei 230026, People's Republic of China
- ⁵⁶ University of South China, Hengyang 421001, People's Republic of China
- ⁵⁷ University of the Punjab, Lahore-54590, Pakistan
- ⁵⁸ (A)University of Turin, I-10125, Turin, Italy; (B)University of Eastern Piedmont, I-15121, Alessandria, Italy; (C)INFN, I-10125, Turin, Italy
- ⁵⁹ Uppsala University, Box 516, SE-75120 Uppsala, Sweden
- ⁶⁰ Wuhan University, Wuhan 430072, People's Republic of China
- ⁶¹ Xinyang Normal University, Xinyang 464000, People's Republic of China
- ⁶² Zhejiang University, Hangzhou 310027, People's Republic of China
- ⁶³ Zhengzhou University, Zhengzhou 450001, People's Republic of China
- ^a Also at Bogazici University, 34342 Istanbul, Turkey
- ^b Also at the Moscow Institute of Physics and Technology, Moscow 141700, Russia
- ^c Also at the Functional Electronics Laboratory, Tomsk State University, Tomsk, 634050, Russia
- ^d Also at the Novosibirsk State University, Novosibirsk, 630090, Russia
- ^e Also at the NRC "Kurchatov Institute", PNPI, 188300, Gatchina, Russia
- ^f Also at Istanbul Arel University, 34295 Istanbul, Turkey
- ^g Also at Goethe University Frankfurt, 60323 Frankfurt am Main, Germany

^h Also at Key Laboratory for Particle Physics, Astrophysics and Cosmology, Ministry of Education; Shanghai Key Laboratory for Particle Physics and Cosmology; Institute of Nuclear and Particle Physics, Shanghai 200240, People's Republic of China

ⁱ Also at Government College Women University, Sialkot - 51310. Punjab, Pakistan.

^j Also at Key Laboratory of Nuclear Physics and Ion-beam Application (MOE) and Institute of Modern Physics, Fudan University, Shanghai 200443, People's Republic of China

^k Also at Harvard University, Department of Physics, Cambridge, MA, 02138, USA

^l Also at State Key Laboratory of Nuclear Physics and Technology, Peking University, Beijing 100871, People's Republic of China

We report the most precise measurements to date of the strong-phase parameters between D^0 and \bar{D}^0 decays to $K_{S,L}^0\pi^+\pi^-$ using a sample of 2.93 fb^{-1} of e^+e^- annihilation data collected at a center-of-mass energy of 3.773 GeV with the BESIII detector at the BEPCII collider. Our results provide the key inputs for a binned model-independent determination of the Cabibbo-Kobayashi-Maskawa angle γ/ϕ_3 with B decays. Using our results, the decay model sensitivity to the γ/ϕ_3 measurement is expected to be between 0.7° and 1.2° , approximately a factor of three smaller than that achievable with previous measurements. The improved precision of this work ensures that measurements of γ/ϕ_3 will not be limited by knowledge of strong phases for the next decade. Furthermore, our results provide critical input for other flavor-physics investigations, including charm mixing, other measurements of CP violation, and the measurement of strong-phase parameters for other D -decay modes.

PACS numbers: 13.25.Ft, 14.40.Lb, 14.65.Dw

The mechanism of CP violation in particle physics is of primary importance because of its impact on cosmological baryogenesis and matter-antimatter asymmetry in the universe. In the standard model (SM), CP violation is studied by measuring the elements of the Cabibbo-Kobayashi-Maskawa (CKM) matrix [1], using the convenient representation given by the unitarity triangle (UT) formed in the complex plane. The angle γ (also denoted ϕ_3) of the UT is of particular interest since it is the only one that can be extracted from tree-level processes, for which the contribution of non-SM effects is expected to be very small. Therefore, measurement of γ provides a benchmark for the SM with minimal theoretical uncertainty [2, 3]. A precision measurement of γ is an essential ingredient in comprehensive testing of the SM description of CP violation and probing for evidence of new physics. Direct measurements of γ have not yet achieved the required precision, with a world-average value of $\gamma = (73.5_{-5.1}^{+4.2})^\circ$ [4], to be compared to the indirect determination of $\gamma = (65.8_{-1.7}^{+1.0})^\circ$ [5]. These different determinations deviate by 1.5σ . It has been predicted that new physics at the tree level could introduce a deviation in γ up to 4° [6], which is close to the current experimental precision. Achieving sub-degree precision in the determination of γ is clearly a top priority for current and future flavor-physics experiments.

One of the most sensitive decay channels for measuring γ is $B^- \rightarrow DK^-$ with $D \rightarrow K_S^0\pi^+\pi^-$ [7], where D represents a superposition of D^0 and \bar{D}^0 mesons. (Throughout this paper, charge conjugation is assumed unless otherwise explicitly noted.) The model-independent approach [8] requires a binned Dalitz plot analysis of the amplitude-weighted average cosine and sine of the relative strong-phase ($\Delta\delta_D$) between D^0 and $\bar{D}^0 \rightarrow K_S^0\pi^+\pi^-$ to determine γ . These strong-phase parameters were first studied by the CLEO collaboration using 0.82 fb^{-1} of data [9, 10]. The limited precision of CLEO's results contributes a systematic uncertainty of approximately 4° to the γ measurement [11], currently the dominant systematic limitation in this determination. In the coming decades, the statistical uncertainties of measuring γ will be greatly reduced

by LHCb and Belle II, potentially to 1° or less. The model-independent approach provides the most precise stand-alone γ measurement [11], and therefore improved measurements of the D strong-phase parameters are essential in maximizing the precision of γ from these future data sets.

In this Letter, we use the model-independent approach of Ref. [8] for the determination of the strong-phase parameters between D^0 and $\bar{D}^0 \rightarrow K_{S,L}^0\pi^+\pi^-$. More details are presented in a companion paper submitted to Physical Review D [13]. Our data sample was collected from e^+e^- annihilations at $\sqrt{s} = 3.773\text{ GeV}$, just above the energy threshold for production of $D\bar{D}$ events. At this energy we take advantage of unique quantum correlations afforded by production through the $\psi(3770)$ resonance. The total integrated luminosity of our sample is 2.93 fb^{-1} [14], 3.6 times that of the CLEO measurement. The expected improvement in precision of the strong-phase parameters will significantly reduce the uncertainties of determinations of γ [11, 15–18] that utilize $D \rightarrow K_{S,L}^0\pi^+\pi^-$. Additionally, improved knowledge of these strong-phase parameters will have significant impact in other applications, including measurements of the CKM angle β (also denoted ϕ_1) through time-dependent analyses of $B^0 \rightarrow Dh^0$ [19] (where h is a light meson) and $B^0 \rightarrow D\pi^+\pi^-$ [20], as well as measurements of charm mixing and CP violation [21–24].

For this study we analyze the $D \rightarrow K_S^0\pi^+\pi^-$ Dalitz plot phase space of m_-^2 vs. m_+^2 , where m_-^2 and m_+^2 are the squared invariant masses of the $K_S^0\pi^-$ and $K_S^0\pi^+$, respectively. The phase space is partitioned into eight pairs of irregularly shaped bins following the three schemes defined in Ref. [10], which are divided according to regions of similar strong-phase difference $\Delta\delta_D$ or maximum sensitivity to γ in the presence of negligible (significant) background; here these schemes are referred to as “equal $\Delta\delta_D$ ” and “(modified) optimal”, respectively. The bin index i ranges from -8 to 8 (excluding 0), with the bins symmetric under the exchange $m_-^2 \leftrightarrow m_+^2$ ($i \leftrightarrow -i$). The strong-phase parameters are denoted c_i and s_i , where c_i is the amplitude-weighted average of $\cos\Delta\delta_D$ in the i th region

of the Dalitz plot (\mathcal{D}_i) and is given by

$$c_i = \frac{\int_{\mathcal{D}_i} |\mathcal{A}| |\bar{\mathcal{A}}| \cos \Delta \delta_D d\mathcal{D}}{\sqrt{\int_{\mathcal{D}_i} |\mathcal{A}|^2 d\mathcal{D} \int_{\mathcal{D}_i} |\bar{\mathcal{A}}|^2 d\mathcal{D}}}, \quad (1)$$

where \mathcal{A} is the amplitude for $D^0 \rightarrow K_S^0 \pi^+ \pi^-$ over the Dalitz plot. The term s_i is defined analogously, with $\cos \Delta \delta_D$ replaced by $\sin \Delta \delta_D$. Because the effects of charm mixing and CP violation in the D decay are negligible, we take $c_i = c_{-i}$ and $s_i = -s_{-i}$. The measurement involves studying the density of the correlated $D \rightarrow K_S^0 \pi^+ \pi^-$ vs. $D \rightarrow K_{S,L}^0 \pi^+ \pi^-$ Dalitz plots, as well as decays of a D meson tagged in a CP eigenstate decaying to $K_{S,L}^0 \pi^+ \pi^-$. The expected yields can be expressed in terms of the parameters K_i , c_i and s_i for $D^0 \rightarrow K_S^0 \pi^+ \pi^-$, and K'_i , c'_i and s'_i for $D \rightarrow K_L^0 \pi^+ \pi^-$, where $K_i^{(\prime)}$ is determined from the distribution of the flavor-tagged $D^0 \rightarrow K_{S,L}^0 \pi^+ \pi^-$ decays across the bins of the Dalitz plot as $K_i^{(\prime)} = h_D \int_{\mathcal{D}_i} |\mathcal{A}|^2 d\mathcal{D}$ and h_D is a normalization factor. Therefore, the strong-phase parameters c_i , s_i , c'_i , and s'_i can be determined by minimizing the likelihood function constructed from the observed and expected yields of these decays.

Details about the BESIII detector design and performance are provided in Ref. [25]. Signal efficiencies and background yields are determined from simulated Monte Carlo (MC) events that are processed identically to data. The generation of simulated samples for the signal processes $D^0 \rightarrow K_S^0 \pi^+ \pi^-$ and $D^0 \rightarrow K_L^0 \pi^+ \pi^-$ are based on measured isobar resonance amplitudes from the Dalitz plot of $D^0 \rightarrow K_S^0 \pi^+ \pi^-$.

To measure strong-phase parameters, we select ‘‘single-tag’’ (ST) and ‘‘double-tag’’ (DT) samples as listed in Table I. STs are D mesons reconstructed from their daughter particles in one of 17 decay modes, of which four are flavor-specific, five are CP -even, seven are CP -odd, and one ($K_S^0 \pi^+ \pi^-$) is CP -mixed. Note that we count $D \rightarrow \pi^+ \pi^- \pi^0$ as a CP -even eigenstate while explicitly correcting for its small CP -odd component [26]. DTs are events with an ST and a second D meson reconstructed as either $K_S^0 \pi^+ \pi^-$ or $K_L^0 \pi^+ \pi^-$. The K_L^0 mesons are not directly reconstructed and their presence is inferred by partial reconstruction technique where one particle is identified by the missing energy and mass in the event. DTs are only formed in combinations where there is a maximum of one unreconstructed particle.

The selection and yield determination procedures of ST and DT candidates are described in the companion article [13] and are summarized below. The ST D signals are identified using the beam-constrained mass $M_{BC} = \sqrt{(\sqrt{s}/2)^2 - |\vec{p}_{D_{\text{tag}}}|^2}$ and $\Delta E = \sqrt{s}/2 - E_{D_{\text{tag}}}$, where $\vec{p}_{D_{\text{tag}}}$ and $E_{D_{\text{tag}}}$ are the momentum and energy of the D candidate, respectively. The ST yields are obtained by performing maximum likelihood fits to M_{BC} distributions. For decay modes that cannot be fully reconstructed ($K^+ e^- \bar{\nu}_e$, $K_L^0 \pi^0$ and $K_L^0 \pi^0 \pi^0$), the ST yields are estimated with the number of neutral $D\bar{D}$ events in data [27], the decay branching fractions [4] and ST efficiencies determined with MC simulation. The ST yields, N_{ST} , are listed in the second column of Table I.

TABLE I. Summary of ST yields (N_{ST}) and DT yields for $K_{S,L}^0 \pi^+ \pi^-$ vs. various tags. The uncertainties are statistical only. The tag modes of $\pi^+ \pi^- \pi^0$, $K_S^0 \eta'$, $K_L^0 \pi^0 \pi^0$ and the partially-reconstructed $K_S^0 \pi^+ \pi^-$ events are used for the first time.

Mode	N_{ST}	$N_{K_S^0 \pi^+ \pi^-}^{DT}$	$N_{K_L^0 \pi^+ \pi^-}^{DT}$
Flavor tags			
$K^+ \pi^-$	549373 ± 756	4740 ± 71	9511 ± 115
$K^+ \pi^- \pi^0$	1076436 ± 1406	5695 ± 78	11906 ± 132
$K^+ \pi^- \pi^- \pi^+$	712034 ± 1705	8899 ± 95	19225 ± 176
$K^+ e^- \bar{\nu}_e$	458989 ± 5724	4123 ± 75	
CP-even tags			
$K^+ K^-$	57050 ± 231	443 ± 22	1289 ± 41
$\pi^+ \pi^-$	20498 ± 263	184 ± 14	531 ± 28
$K_S^0 \pi^0 \pi^0$	22865 ± 438	198 ± 16	612 ± 35
$\pi^+ \pi^- \pi^0$	107293 ± 716	790 ± 31	2571 ± 74
$K_L^0 \pi^0$	103787 ± 7337	913 ± 41	
CP-odd tags			
$K_S^0 \pi^0$	66116 ± 324	643 ± 26	861 ± 46
$K_S^0 \eta_{\gamma\gamma}$	9260 ± 119	89 ± 10	105 ± 15
$K_S^0 \eta_{\pi^+ \pi^- \pi^0}$	2878 ± 81	23 ± 5	40 ± 9
$K_S^0 \omega$	24978 ± 448	245 ± 17	321 ± 25
$K_S^0 \eta'_{\pi^+ \pi^- \eta}$	3208 ± 88	24 ± 6	38 ± 8
$K_S^0 \eta'_{\gamma\pi^+ \pi^-}$	9301 ± 139	81 ± 10	120 ± 14
$K_L^0 \pi^0 \pi^0$	50531 ± 6128	620 ± 32	
Mixed CP tags			
$K_S^0 \pi^+ \pi^-$	188912 ± 756	899 ± 31	3438 ± 72
$K_S^0 \pi^+ \pi^-_{\text{miss}}$		224 ± 17	
$K_S^0 (\pi^0 \pi^0_{\text{miss}}) \pi^+ \pi^-$		710 ± 34	

The yields of DT candidates consisting of $K_S^0 \pi^+ \pi^-$ vs. fully reconstructed final states are determined with a two-dimensional unbinned maximum-likelihood fit to the M_{BC}^{sig} (signal) vs. M_{BC}^{tag} (tag) distribution. The DT candidates with an undetectable neutrino or K_L^0 are reconstructed by combining a $K_S^0 \pi^+ \pi^-$ candidate with the remaining charged or neutral particles, that are assigned to the other D decay. The variable $U_{\text{miss}} = E_{\text{miss}} - |\vec{p}_{\text{miss}}|$ (for $K^+ e^- \bar{\nu}_e$) or missing-mass squared (M_{miss}^2) are calculated from the missing energy and momentum in the event. To reduce background contributions, events with excess neutral energy or charged tracks are rejected.

The $K_S^0 \pi^+ \pi^-$ vs. $K_S^0 \pi^+ \pi^-$ DTs are crucial for determining the s_i values, and thus in order to increase the yield for these events, we include two types of partially reconstructed events, which more than doubles the yield. The first ($K_S^0 \pi^\pm \pi_{\text{miss}}^\mp$) allows for one pion originating from the D meson to be unreconstructed in the detector. For these events, which have only three charged tracks recoiling against the $D \rightarrow K_S^0 \pi^+ \pi^-$ ST, the missing pion is inferred from the M_{miss}^2 of the event. The second ($K_S^0 (\pi^0 \pi^0_{\text{miss}}) \pi^+ \pi^-$) is the case where one K_S^0 meson decays to $\pi^0 \pi^0$, with only one π^0 detected while the other π^0 is undetected. We select events with only two additional oppositely charged tracks recoiling against the $D \rightarrow K_S^0 \pi^+ \pi^-$ ST and identify these as the π^+ and π^- from the other D meson. The resulting distributions

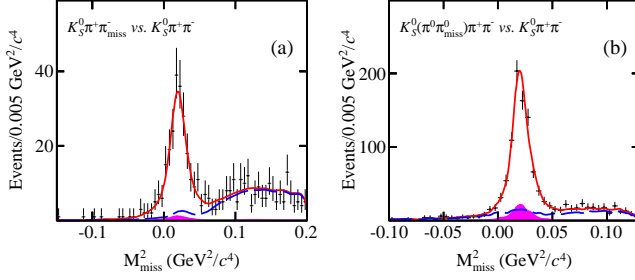


FIG. 1. Fits to M_{miss}^2 distributions in data. Points with error bars are data, long-dashed (blue) curves are the fitted combinatorial backgrounds. The shaded areas (pink) show MC estimates of the peaking backgrounds from (a) $D \rightarrow \pi^+ \pi^- \pi^+ \pi^-$ and (b) $D \rightarrow \pi^+ \pi^- \pi^0 \pi^0$, and the red solid curves are the total fits.

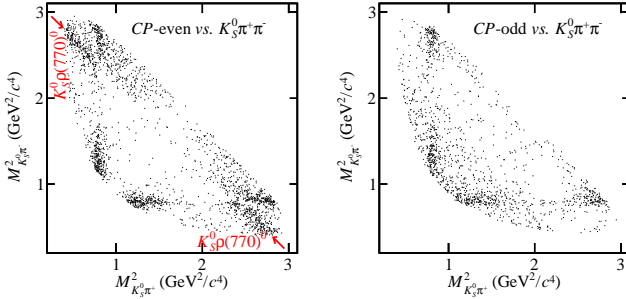


FIG. 2. Dalitz plots of $K_S^0 \pi^+ \pi^-$ events in data. The effect of the quantum correlation is clearly visible. The approximate locations of events from $K_S^0 \rho(770)^0$ are indicated by arrows for clarity.

of M_{miss}^2 show clear signals with minimal background, and signal yields are obtained with unbinned maximum-likelihood fits, as is shown in Fig. 1.

The DT yields of $K_S^0 \pi^+ \pi^-$ and $K_L^0 \pi^+ \pi^-$ tagged by different channels are shown in the third and fourth columns of Table I, respectively. Overall, the DT yields of $D \rightarrow K_{S(L)}^0 \pi^+ \pi^-$ involving a CP eigenstate are a factor of 5.3 (9.2) larger than those in Ref. [10], and the DT yields of $K_S^0 \pi^+ \pi^-$ tagged with $D \rightarrow K_{S(L)}^0 \pi^+ \pi^-$ decays are a factor of 3.9 (3.0) larger than those in Ref. [10]. These increases come not only from the larger data set available at BESIII but also from the additional tag modes and the application of partial-reconstruction techniques. Figure 2 shows the Dalitz plots of CP -even and CP -odd tagged $D \rightarrow K_S^0 \pi^+ \pi^-$ events selected in the data. The effect of quantum correlations arising from production through $\psi(3770) \rightarrow D^0 \bar{D}^0$ is demonstrated by the differences between these plots. Most noticeably, the CP -odd component $K_S^0 \rho(770)^0$ is visible in CP -even tagged $K_S^0 \pi^+ \pi^-$ samples but absent from CP -odd samples.

The DT yield for the i th bin of the Dalitz plot of each tagged $D \rightarrow K_{S(L)}^0 \pi^+ \pi^-$ sample, N_i^{obs} , can be determined by fitting the DT events observed in this bin. Here the yield includes the signal and any peaking background component. The expected DT yields in the i th bin of Dalitz plot of each

tagged $D \rightarrow K_{S(L)}^0 \pi^+ \pi^-$ sample, N_i^{exp} , are sums of the expected signal yields and the expected peaking backgrounds. It should be noted that detector resolution effects can cause individual events to migrate between Dalitz plot bins after reconstruction. Such migration effects vary among bins due to the irregular bin shapes, coupled with the rapid variations of the Dalitz plot density. Furthermore, migrations differ between $D \rightarrow K_S^0 \pi^+ \pi^-$ and $D \rightarrow K_L^0 \pi^+ \pi^-$ decays due to different resolutions in the Dalitz plots ($0.0068 \text{ GeV}^2/c^4$ for $D \rightarrow K_S^0 \pi^+ \pi^-$ and $0.0105 \text{ GeV}^2/c^4$ for $D \rightarrow K_L^0 \pi^+ \pi^-$). The resultant bin migrations range within (3-12)% and (3-18)% for the $K_S^0 \pi^+ \pi^-$ and $K_L^0 \pi^+ \pi^-$ signals, respectively. Therefore, in the determination of the DT yields, simulated efficiency matrices are introduced to account for bin migration and reconstruction efficiencies [13]. Studies indicate that neglecting bin migration introduces biases in the determination of c_i (s_i) that average a factor of 0.7 (0.3) times the statistical uncertainty of this analysis, so it is important to correct for this effect. The values of K_i and K'_i that are used to evaluate N_i^{exp} are determined from the flavor-tagged DT yields, where corrections from doubly Cabibbo-suppressed decays, efficiency and migration effects have been applied, which are explained in detail in Ref. [13].

The values of $c_i^{(l)}$ and $s_i^{(l)}$ are obtained by minimizing the negative log-likelihood function constructed as

$$-2 \log \mathcal{L} = -2 \sum_i \sum_j \ln P(N_{ij}^{\text{obs}}, \langle N_{ij}^{\text{exp}} \rangle)_{K_S^0 \pi^+ \pi^-, K_{S(L)}^0 \pi^+ \pi^-} - 2 \sum_i \ln P(N_i^{\text{obs}}, \langle N_i^{\text{exp}} \rangle)_{CP, K_{S(L)}^0 \pi^+ \pi^-} + \chi^2,$$

where $P(N^{\text{obs}}, \langle N^{\text{exp}} \rangle)$ is the Poisson probability to observe N^{obs} events given the expected number $\langle N^{\text{exp}} \rangle$. Here the sums are over the bins of the $D^0 \rightarrow K_{S(L)}^0 \pi^+ \pi^-$ Dalitz plots. The χ^2 term is used to constrain the difference $c'_i - c_i$ ($s'_i - s_i$) to the predicted quantity Δc_i (Δs_i). The values of Δc_i and Δs_i are estimated based on the decay amplitudes of $D^0 \rightarrow K_S^0 \pi^+ \pi^-$ [28] and $D^0 \rightarrow K_L^0 \pi^+ \pi^-$, where the latter is constructed by adjusting the $D^0 \rightarrow K_S^0 \pi^+ \pi^-$ model taking the K_S^0 and K_L^0 mesons to have opposite CP , as is discussed in Refs. [9, 10]. The details of assigning Δc_i (Δs_i) and their uncertainties $\delta \Delta c_i$ ($\delta \Delta s_i$) are presented in Table VI of Ref. [13].

The measured strong-phase parameters $c_i^{(l)}$ and $s_i^{(l)}$ are presented in Fig. 3 and Table II. Their systematic uncertainties arise from the evaluation of K_i and K'_i , the estimation of ST yields, the MC statistics, subtraction of the DT peaking background, the fitting procedure for determining DT yields, the difference in momentum resolution between data and MC simulation, and the effects of $D^0 \bar{D}^0$ mixing. The estimation of these systematic uncertainties is described in detail in Ref. [13]. In addition to our results, Fig. 3 includes the predictions of Ref. [28] and the results from Ref. [10], which show reasonable agreement.

In summary, measurements of the strong-phase parameters between D^0 and $\bar{D}^0 \rightarrow K_{S,L}^0 \pi^+ \pi^-$ in bins of phase space have been performed using 2.93 fb^{-1} of data collected at $\sqrt{s}=3.773 \text{ GeV}$ with the BESIII detector. Compared to the

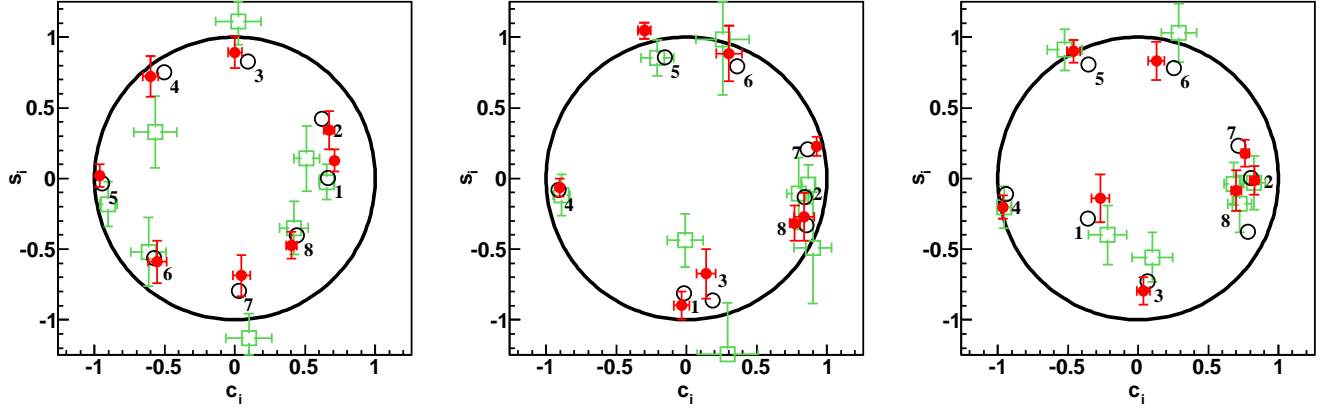


FIG. 3. The c_i and s_i measured in this work (red dots with error bars), the predictions of Ref. [28] (black open circles) and the results of Ref. [10] (green open squares with error bars). The left, middle and right plots are from the equal $\Delta\delta_D$, optimal and modified optimal binnings, respectively. The circle indicates the boundary of the physical region $c_i^2 + s_i^2 = 1$.

previous CLEO measurement [10], two main improvements have been incorporated. First, additional tag decay modes are used. In particular the inclusion of the $\pi^+\pi^-\pi^0$ tag improves the sensitivity to c_i and the addition of the $K_S^0(\pi^0\pi_{\text{miss}}^0)\pi^+\pi^-$ improves the sensitivity to s_i . Second, corrections for bin migration have been included, as their neglect would lead to uncertainties comparable to the statistical uncertainty. The results presented in this Letter are on average a factor of 2.5 (1.9) more precise for c_i (s_i) and a factor of 2.8 (2.2) more precise for c'_i (s'_i) than has been achieved previously. The strong-phase parameters provide an important input for a wide range of CP violation measurements in the beauty and charm sectors, and also for measurements of strong-phase parameters in other D decays where $D \rightarrow K_S^0\pi^+\pi^-$ is used as a tag [29–33].

To assess the impact of our c_i and s_i results on a measurement of γ , we use a large simulated data set of $B^- \rightarrow DK^-$, $D \rightarrow K_S^0\pi^+\pi^-$ events. These are generated with the expected distribution given for our measured central values of K_i , c_i , and s_i and the input values $\gamma = 73.5^\circ$, $r_B = 0.103$, and $\delta_B = 136.9^\circ$ [34], where r_B is the ratio of the suppressed amplitude to the favored amplitude and δ_B is their strong-phase difference. The simulated data are fitted 10,000 times to determine γ , δ_B and r_B . The values of c_i and s_i used in each fit are sampled from the measured values smeared by their uncertainties accounting for any correlations. Based on this study, the uncertainty in γ associated with our uncertainties for c_i and s_i is found to be 0.7° , 1.2° and 0.8° for the equal $\Delta\delta_D$, optimal and modified optimal binning schemes, respectively. For comparison, the corresponding results from CLEO are 2.0° , 3.9° and 2.1° [10]. Therefore, the uncertainty on γ arising from knowledge of the charm strong phases is approximately a factor of three smaller than was possible with the CLEO measurements.

For the first time, the dominant systematic uncertainty for γ measurement from the strong-phase parameters will be constrained to around 1° , or less, for γ measurements with future

B experiments [11, 15–18]. The predicted statistical uncertainties on γ from LHCb prior to the start of High-Luminosity LHC operation in the mid 2020s, and from Belle II are expected to be around 1.5° [35, 36]. The improved precision achieved here will ensure that measurements of γ from LHCb and Belle II over the next decade are not limited by the knowledge of these strong-phase parameters.

The BESIII collaboration thanks the staff of BEPCII and the IHEP computing center for their strong support. This work is supported in part by National Key Basic Research Program of China under Contract No. 2015CB856700; National Natural Science Foundation of China (NSFC) under Contracts Nos. 11625523, 11635010, 11735014, 11775027, 11822506, 11835012; the Chinese Academy of Sciences (CAS) Large-Scale Scientific Facility Program; Joint Large-Scale Scientific Facility Funds of the NSFC and CAS under Contracts Nos. U1532257, U1532258, U1732263, U1832207; CAS Key Research Program of Frontier Sciences under Contracts Nos. QYZDJ-SSW-SLH003, QYZDJ-SSW-SLH040; 100 Talents Program of CAS; INPAC and Shanghai Key Laboratory for Particle Physics and Cosmology; ERC under Contract No. 758462; German Research Foundation DFG under Contracts Nos. Collaborative Research Center CRC 1044, FOR 2359; Istituto Nazionale di Fisica Nucleare, Italy; Koninklijke Nederlandse Akademie van Wetenschappen (KNAW) under Contract No. 530-4CDP03; Ministry of Development of Turkey under Contract No. DPT2006K-120470; National Science and Technology fund; STFC (United Kingdom); The Knut and Alice Wallenberg Foundation (Sweden) under Contract No. 2016.0157; The Royal Society, UK under Contracts Nos. DH140054, DH160214; The Swedish Research Council; U. S. Department of Energy under Contracts Nos. DE-FG02-05ER41374, DE-SC-0010118, DE-SC-0012069; University of Groningen (RuG) and the Helmholtzzentrum fuer Schwerionenforschung GmbH (GSI), Darmstadt; This paper is also supported by Beijing municipal government under Contract No CIT&TCD201704047, and by the Royal Society under Contract No. NF170002.

TABLE II. The measured strong-phase parameters $c_i^{(\prime)}$ and $s_i^{(\prime)}$, where the first uncertainties are statistical and the second are systematic.

	Equal $\Delta\delta_D$ binning		Optimal binning		Modified optimal binning	
	c_i	s_i	c_i	s_i	c_i	s_i
1	0.708(0.020)(0.009)	0.128(0.076)(0.017)	-0.034(0.052)(0.017)	-0.899(0.094)(0.030)	-0.270(0.061)(0.019)	-0.140(0.168)(0.027)
2	0.671(0.035)(0.016)	0.341(0.134)(0.015)	0.839(0.062)(0.037)	-0.272(0.166)(0.031)	0.829(0.027)(0.018)	-0.014(0.100)(0.018)
3	0.001(0.047)(0.019)	0.893(0.112)(0.019)	0.140(0.064)(0.028)	-0.674(0.172)(0.037)	0.038(0.044)(0.021)	-0.796(0.095)(0.020)
4	-0.602(0.053)(0.016)	0.723(0.143)(0.015)	-0.904(0.021)(0.009)	-0.065(0.062)(0.006)	-0.963(0.020)(0.009)	-0.202(0.080)(0.014)
5	-0.965(0.019)(0.013)	0.020(0.081)(0.009)	-0.300(0.042)(0.013)	1.047(0.055)(0.014)	-0.460(0.044)(0.011)	0.899(0.078)(0.013)
6	-0.554(0.062)(0.024)	-0.589(0.147)(0.030)	0.303(0.088)(0.027)	0.884(0.191)(0.042)	0.130(0.055)(0.017)	0.832(0.131)(0.029)
7	0.046(0.057)(0.023)	-0.686(0.143)(0.028)	0.927(0.016)(0.008)	0.228(0.066)(0.015)	0.762(0.025)(0.012)	0.178(0.094)(0.016)
8	0.403(0.036)(0.017)	-0.474(0.091)(0.027)	0.771(0.032)(0.015)	-0.316(0.123)(0.020)	0.699(0.035)(0.012)	-0.085(0.141)(0.018)
	c_i'	s_i'	c_i'	s_i'	c_i'	s_i'
1	0.801(0.020)(0.013)	0.137(0.078)(0.016)	0.240(0.054)(0.015)	-0.854(0.106)(0.032)	-0.198(0.067)(0.025)	-0.209(0.181)(0.027)
2	0.848(0.036)(0.016)	0.279(0.137)(0.016)	0.927(0.054)(0.036)	-0.298(0.162)(0.029)	0.945(0.026)(0.018)	-0.019(0.100)(0.017)
3	0.174(0.047)(0.016)	0.840(0.118)(0.020)	0.742(0.060)(0.030)	-0.350(0.180)(0.039)	0.477(0.040)(0.019)	-0.709(0.119)(0.028)
4	-0.504(0.055)(0.019)	0.784(0.147)(0.014)	-0.930(0.023)(0.019)	-0.075(0.075)(0.007)	-0.948(0.021)(0.013)	-0.235(0.086)(0.014)
5	-0.972(0.021)(0.017)	-0.008(0.089)(0.009)	-0.173(0.043)(0.010)	1.053(0.062)(0.016)	-0.359(0.046)(0.011)	0.943(0.084)(0.013)
6	-0.387(0.069)(0.025)	-0.642(0.152)(0.033)	0.554(0.073)(0.032)	0.605(0.184)(0.042)	0.333(0.051)(0.019)	0.701(0.137)(0.028)
7	0.462(0.056)(0.019)	-0.550(0.159)(0.030)	0.975(0.017)(0.008)	0.198(0.071)(0.014)	0.878(0.026)(0.015)	0.188(0.098)(0.016)
8	0.640(0.036)(0.015)	-0.399(0.099)(0.026)	0.798(0.035)(0.017)	-0.253(0.141)(0.019)	0.740(0.037)(0.014)	-0.025(0.149)(0.019)

- [1] N. Cabibbo, Phys. Rev. Lett. **10**, 531 (1963); M. Kobayashi and T. Maskawa, Prog. Theor. Phys. **49**, 652 (1973).
- [2] J. Brod and J. Zupan, J. High Energy Phys. **01** (2014) 051.
- [3] M. Blanke and A. Buras, Eur. Phys. J. C **79**, 159 (2019).
- [4] M. Tanabashi *et al.* (Particle Data Group), Phys. Rev. D **98**, 030001 (2018).
- [5] J. Charles *et al.* (CKMfitter Group), Eur. Phys. J. C **41**, 1 (2005); and updates at <http://ckmfitter.in2p3.fr>; M. Bona *et al.* (UTfit Collaboration), J. High Energy Phys. **07** (2005) 028; and updates at <http://utfit.org/UTfit/WebHome>.
- [6] J. Brod, A. Lenz, G. Tetlalmatzi-Xolocotzi and M. Wiebusch, Phys. Rev. D **92**, 033002 (2015).
- [7] A. Giri, Y. Grossman, A. Soffer, and J. Zupan, Phys. Rev. D **68**, 054018 (2003).
- [8] A. Bondar and A. Poluektov, Eur. Phys. J. C **47**, 347 (2006); Eur. Phys. J. C **55**, 51 (2008).
- [9] R. A. Briere *et al.* (CLEO Collaboration), Phys. Rev. D **80**, 032002 (2009).
- [10] J. Libby *et al.* (CLEO Collaboration), Phys. Rev. D **82**, 112006 (2010).
- [11] R. Aaij *et al.* (LHCb Collaboration), J. High Energy Phys. **08** (2018) 176; Erratum: J. High Energy Phys. **08** (2018) 107.
- [12] A. Cerri, V.V. Gligorov, S. Malvezzi, J. M. Camalich, J. Zupan *et al.*, CERN Yellow Rep. Monogr. **7**, (2019) 867; arXiv:1812.07638.
- [13] M. Ablikim *et al.* (BESIII Collaboration), submitted to PRD, arXiv:xxxx.
- [14] M. Ablikim, *et al.* (BESIII Collaboration), Chin. Phys. C **37**, 123001 (2013); Phys. Lett. B **753**, 629 (2016).
- [15] R. Aaij *et al.* (LHCb Collaboration), Phys. Lett. B **718**, 43 (2012).
- [16] R. Aaij *et al.* (LHCb Collaboration), J. High Energy Phys. **10** (2014) 097.
- [17] R. Aaij *et al.* (LHCb Collaboration), J. High Energy Phys. **06** (2016) 131.
- [18] H. Aihara *et al.* (Belle Collaboration), Phys. Rev. D **85**, 112014 (2012).
- [19] V. Vorobyev *et al.* (Belle Collaboration), Phys. Rev. D **94**, 052004 (2016).
- [20] A. Bondar, A. Kuzmina and V. Vorobyev, J. High Energy Phys. **03** (2018) 195.
- [21] C. Thomas and G. Wilkinson, J. High Energy Phys. **10** (2012) 185.
- [22] R. Aaij *et al.* (LHCb Collaboration), J. High Energy Phys. **04** (2016) 033.
- [23] A. Di. Canto, J. Garra Tic, T. Gershon, N. Jurik, M. Martinelli, T. Pila, S. Stahl and D. Tonelli, Phys. Rev. D **99**, 012007 (2019).
- [24] R. Aaij *et al.* (LHCb Collaboration), Phys. Rev. Lett. **122**, 231802 (2019).
- [25] M. Ablikim *et al.* (BESIII Collaboration), Nucl. Instrum. Methods Phys. Res., Sect. A **614**, 345 (2010).
- [26] S. Malde *et al.*, Phys. Lett. B **747**, 9 (2015).
- [27] M. Ablikim, *et al.* (BESIII Collaboration), Chin. Phys. C **42**, 083001 (2018).
- [28] I. Adachi *et al.* (BaBar and Belle Collaborations), Phys. Rev. D **98**, 110212 (2018).
- [29] M. Nayak *et al.*, Phys. Lett. B **747**, 9 (2015).
- [30] S. Harnew, P. Naik, C. Prouve, J. Rademacker and D. Asner, J. High Energy Phys. **01** (2018) 144.
- [31] T. Evans, S.T. Harnew, J. Libby, S. Malde, J. Rademacker and G. Wilkinson, Phys. Lett. B. **757**, 520 (2016).
- [32] J. Insler *et al.* (CLEO Collaboration), Phys. Rev. D **85**, 092016 (2012).
- [33] P. K. Resmi, J. Libby, S. Malde and G. Wilkinson, J. High Energy Phys. **01** (2018) 082.
- [34] Y. Amhis *et al.*, (Heavy Flavor Averaging Group), Eur. Phys. J. C **77**, 895 (2017); and updates at <https://hflav.web.cern.ch>.
- [35] I. Bediaga *et al.* (LHCb Collaboration), HCB-PUB-2018-009, CERN-LHCC-2018-027 [arXiv:1808.08865].
- [36] E. Kou *et al.* (Belle II Collaboration), KEK Preprint 2018-27, BELLE2-PUB-PH-2018-001, FERMILAB-PUB-18-398-T, JLAB-THY-18-2780, INT-PUB-18-047, UWThPh 2018-26 [arXiv:1808.10567].